

Design and demonstration of high efficiency anti-glare LED luminaires for indoor lighting

Che-Wen Chiang,¹ Yu-Kai Hsu,⁴ and Jui-Wen Pan^{1,2,3,*}

¹Institute of Photonic System, National Chiao Tung University, Tainan City 71150, Taiwan

²Biomedical Electronics Translational Research Center, National Chiao Tung University, Hsin-Chu City 30010, Taiwan

³Department of Medical Research, Chi Mei Medical Center, Tainan 71004, Taiwan

⁴Institute of Lighting and Energy Photonics, National Chiao Tung University, Tainan City 71150, Taiwan
[*juiwenpan@gmail.com](mailto:juiwenpan@gmail.com)

Abstract: An anti-glare luminaire design is proposed to reduce the effect of glare and the multi-shadow while preserving high optical efficiency, high illumination uniformity and low unified glare rating (UGR). Comparison to the traditional direct light emitting diode (LED) luminaire in optical simulations showed an enhancement of the illumination uniformity from 64.9% to 80.0%. The optical efficiency was 79.5%, and the UGR value was controlled under 18.8. For the actual measurement, the finished product had an illumination uniformity of 77.0%, optical efficiency of 76.0%, UGR value of 19.0, and efficacy of 81.4 lm/w. Through this design, the lighting performance was greatly enhanced.

©2014 Optical Society of America

OCIS codes: (220.4830) Systems design; (230.3670) Light-emitting diodes; (220.2945) Illumination design; (080.4295) Nonimaging optical systems; (080.4298) Nonimaging optics.

References and links

1. C. H. Tsuei, J. W. Pen, and W. S. Sun, "Simulating the illuminance and the efficiency of the LED and fluorescent lights used in indoor lighting design," *Opt. Express* **16**(23), 18692–18701 (2008).
2. CIE Technical Report 117. "Discomfort glare in interior lighting." Vienna, Austria: CIE, 1995.
3. Osram, "Sireco louver luminaire T8 ribbed matt 3x18W T8 M625 ALU RIB", <http://www.osram.com/>.
4. X. H. Lee, I. Moreno, and C.-C. Sun, "High-performance LED street lighting using microlens arrays," *Opt. Express* **21**(9), 10612–10621 (2013).
5. Cougar Led lighting, "PR48 - 2' x 2' Recessed Direct Panel Light," <http://www.cougar-lighting.com/>
6. *Epoch lighting*, "CL-R345-60W Database," <http://www.lighting-epoch.com/>
7. H. W. Lee and L. B. -S. Lin, "Improvement of illumination uniformity for LED flat panel light by using micro-secondary lens array," *Opt. Express* **20**(S6), A788–A798 (2012).
8. P. Ngai and P. R. Boyce, "The effect of overhead glare on visual discomfort," *J. Illum. Eng. Soc.* **29**(2), 29–38 (2000).
9. Y. Ding, X. Liu, Z. R. Zheng, and P. F. Gu, "Freeform LED lens for uniform illumination," *Opt. Express* **16**(17), 12958–12966 (2008).
10. K. Wang, D. Wu, Z. Qin, F. Chen, X. Luo, and S. Liu, "New reversing design method for LED uniform illumination," *Opt. Express* **19**(S4 Suppl 4), A830–A840 (2011).
11. Y. C. Su and Q. G. Wu, *Numerical Solutions of Partial Differential Equations* (Weather, 1989), Chap. 1.
12. I. Moreno, "Illumination uniformity assessment based on human vision," *Opt. Lett.* **35**(23), 4030–4032 (2010).
13. X. Xunli, M. Zhenqiang, and D. Yang, "The ghost of LED lighting and its solution," *China Light & Lighting* (2010).
14. E. R. Méndez, E. E. García-Guerrero, H. M. Escamilla, A. A. Maradudin, T. A. Leskova, and A. V. Shchegrov, "Photofabrication of random achromatic optical diffusers for uniform illumination," *Appl. Opt.* **40**(7), 1098–1108 (2001).
15. H. Urey and K. D. Powell, "Microlens array-based exit pupil expander for full color display applications," *Proc. SPIE* **5456**, 227–236 (2005).
16. J. Chaves, *Introduction to Nonimaging Optics* (CRC Press, 2008).
17. F. D. Vanderwerf, *Applied Prismatic and Reflective Optics* (SPIE Press, 2010).
18. I. Moreno, M. Avendaño-Alejo, and R. I. Tzonchev, "Designing light-emitting diode arrays for uniform near-field irradiance," *Appl. Opt.* **45**(10), 2265–2272 (2006).
19. R. J. Koschel, "Simplex optimization method for illumination design," *Opt. Lett.* **30**(6), 649–651 (2005).
20. R. J. Koschel, *Illumination Engineering: design with nonimaging optics* (Wiley, 2013), Chap. 7.
21. Osram, "Duris® S5 -GW PSLLS1.EC Datasheet," <http://www.osram-os.com/>
22. F. Yamaguchi, *Curves and Surfaces in Computer Aided Geometric Design* (Springer-Verlag, 1988).

23. W. T. Chien, C. C. Sun, and I. Moreno, "Precise optical model of multi-chip white LEDs," *Opt. Express* **15**(12), 7572–7577 (2007).
24. Photo Research, "PR655 data sheet," <http://www.photoresearch.com/>.
25. LMT, "GO-DS 1600 data sheet," <http://www.lmt.de/>.

1. Introduction

The rapid development of LED in recent years has meant that they are now widely used in our daily life. LEDs are more suitable for general lighting than conventional light sources, offering better performance, because of their advantages of low power consumption, long life, compact size, design flexibility and high color render [1]. In the past few years LED panel lights have become one of the most popular products for indoor lighting. Considering the total cost and the fact that they are environmentally friendly, many consumers prefer LED products to the traditional fluorescent lighting. However, the property of high luminance and the light intensity distribution curve (LIDC) indicate that LED panel lights have serious glare effects. The glare effect causes fatigue to the human eye and loss of concentration. Reducing the glare effect is necessary for the improvement of LED products.

The International Commission on Illumination (CIE) recommends a reduction in the UGR value for indoor lighting in order to alleviate the discomfort caused by glare in interior lighting [2]. The UGR value is an appropriate standard for evaluating glare. In modern times, there are three types of luminaires. The first one is the traditional fluorescent light [3] which has the features of high UGR, low illumination uniformity, and low optical efficiency [4]. The LIDC of the fluorescent light can be controlled by using reflectors and grills on the luminaire. The illumination uniformity and UGR can be improved with the appropriate design, but the optical efficiency is still low. The second type of luminaire is the direct LED light. The direct LED light has a high optical efficiency, high UGR and low illumination uniformity [5]. The goal of diffuser sheet design is to produce a uniform illumination along the output plane of diffuser, and to preserve as much as possible the LIDC designed and produced by anti-glare TIR lens. The last type is the edge-lit LED panel light, which has reached high illumination uniformity, high optical efficiency and acceptable UGR [6]. Through the optical element of the light guide and diffuser sheet modulation, the edge-lit LED light offers steady performance. Among the three types of luminaires, the edge-lit LED panel offers the best tradeoff solution. In one word, it is necessary to improve the optical efficiency of direct anti-glare LED lighting with high illumination uniformity, high optical efficiency and acceptable UGR for indoor lighting.

In this paper, we propose an anti-glare luminaire design with an illumination uniformity that can reach 80%, an optical efficiency that can reach 80%, and UGR value of less than 19.0. This design was set up by the optical software of LightTools and DIALux. A working sample of the lighting fixture was produced. The finished anti-glare luminaire had 77.0% illumination uniformity, 76.0% efficiency, and the UGR was 19.0. These results can be applied to current indoor lighting designs with lighting performance greatly enhanced compared to previous lighting designs.

2. Working principles of the anti-glare luminaire

As shown in Fig. 1, the anti-glare luminaire design is composed of the mechanical luminaire, LED array, anti-glare lens and diffuser sheet. The optical efficiency is defined as the total lamp flux divided by the total LED flux. The optical targets of high illumination uniformity, high optical efficiency and acceptable UGR are expected to be met. The illumination uniformity U_E is defined as [7]

$$U_E = E_{\min} / E_{\text{avg}} \quad , \quad \text{Eq. (1)}$$

where the E_{\min} is minimum illuminance and E_{avg} is average illuminance in the target region. In general, high illumination uniformity is achieved by using a high full width at half maximum (FWHM) angle of the LIDC. However, this causes an enhancement of the UGR values. The

optical efficiency is dependent on the design of the optical element. The anti-glare lens design and the diffuser sheet design enable a trade-off between the three optical targets.

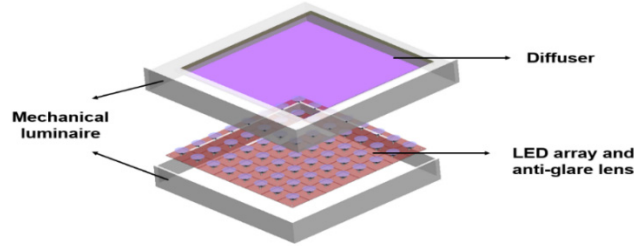


Fig. 1. Illustration of an anti-glare luminaire with anti-glare lens and diffuser sheet.

2.1 An anti-glare lens design

An anti-glare lens is designed for controlling the illumination uniformity and the UGR. The expected LIDC has a batwing distribution with a small FWHM angle. The anti-glare lens is composed of a total internal reflection (TIR) surface and a freeform surface which have different purposes. Through these two main designs, an anti-glare lens with high illumination uniformity and acceptable UGR was constructed.

2.1.1 Geometric analysis of the TIR surface

According to Ngai and Boyce, an uncomfortable glare will occur when the horizontal angle of the luminaire exceeds 53 degrees [8]. In order to reduce this glare effect, the solution is to make the intensity in excess of 53 degrees as low as possible. We can use the anti-glare design to control the LIDC and the glare effect in lighting designs. A TIR surface is a suitable method to control the FWHM angle of the LIDC for LED lighting fixture designs. Moreover, the TIR surface has the advantages of high optical efficiency and convenient manufacturing. There are two critical parameters for geometric analysis of the TIR surface, as shown in Fig. 2. The first one is the radius (R) of the spherical surface and the distance $\overline{O'P}$ between the light emitting surface and the vertex of the sphere. Given the radius and the distance, we decided on a spherical surface. The ray from the LED light source is collimated as it passes through the spherical surface. In the figure, the LED light source is located at O . When the radius R and the $\overline{O'P}$ distance were confirmed, the geometric relationship can be calculated from the cosine theorem as shown in Eq. (2), (3).

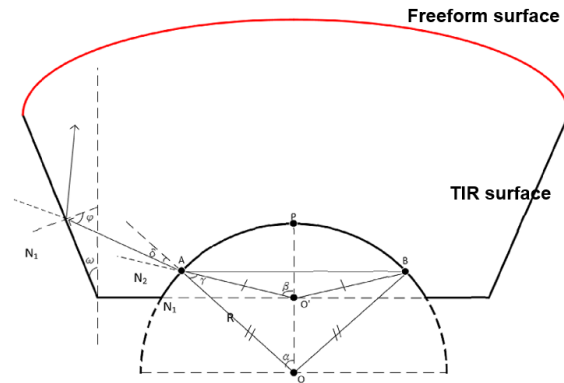


Fig. 2. Geometric illustration of the anti-glare lens

$$(\overline{AB})^2 = R^2 + R^2 - 2R^2 \cos(2\alpha) = (\overline{AO'})^2 + (\overline{AO'})^2 - 2(\overline{AO'})^2 \cos(2\beta), \text{ Eq. (2)}$$

$$(\overline{AO'})^2 = R^2 + (\overline{OO'})^2 - 2R^2(\overline{OO'})^2 \cos \alpha, \quad \text{Eq. (3)}$$

$$\beta = \cos^{-1} \left[1 + \frac{\cos 2\alpha - 1}{1 + \frac{(\overline{OO'})^2}{R^2} - 2 \frac{\overline{OO'}}{R} \cos \alpha} \right], \quad \text{Eq. (4)}$$

$$\gamma = \alpha - \beta, \quad \text{Eq. (5)}$$

$$N_1 \sin \gamma = N_2 \sin \delta, \quad \text{Eq. (6)}$$

$$\varphi = 90^\circ - (\delta + \alpha - \omega), \quad \text{Eq. (7)}$$

Through Eq. (2) and Eq. (3), the relationship between α and β can be expressed as in Eq. (4). Due to the exterior angle formula established in Eq. (5), the angle δ can be calculated by Snell's law in Eq. (6). The LED light source is collimated by the spherical surface. The second critical parameter is the angle of the lens edge (ω). Through a simple geometric calculation, we obtain the angle φ as in Eq. (7). Then, applying the angle φ and Snell's law we calculate the TIR angle. Through collimation from the two surfaces, the FWHM angle of the LIDC will converge less than 53 degrees.

2.1.2 Algorithm for freeform surface design

After controlling glare effect by the TIR surface, the illumination uniformity is another important issue for indoor lighting. Many studies have focused on developing uniform illumination by using light energy mapping [9, 10]. The required LIDC is obtained from the relationship of light energy mapping. Through partial differential equations and numerical methods [11], the geometric relationship of the freeform surface can be calculated and the freeform surface constructed. When the ray passes through the freeform surface of the anti-glare lens, the light energy distribution is balanced at each angle which greatly enhances the uniformity of the illumination.

2.2 Diffuser sheet design for preventing multi-shadow effects

The illumination uniformity and UGR is controlled by the anti-glare lens. However, the luminance of the light emitting surface is not uniform. When looking directly at the LED luminaire there is serious glare effect as well as a multi-shadow effect caused by the LED point light source. The multi-shadow effect generated by different LED light sources makes vision recognition difficult. The luminance uniformity (U_L) [12] (is defined as following:

$$U_L = L_{\min} / L_{\max}, \quad \text{Eq. (8)}$$

where the L_{\min} is minimum luminance and L_{\max} is maximum luminance in the target region. In order to reduce the multi-shadow effect, the luminance uniformity of the emitting surface should be higher than 73.5% [13]. In order to improve luminance uniformity, many different diffuser designs and working principles have been proposed [14–17]. Based on past research studies, we develop a double sided structural diffuser sheet to extend the emitting area of the LED as shown in Fig. 3(a). The diffuser sheet is constructed based on a prism structure and a cylindrical structure [18]. As shown in the Fig. 3(b)-1, the luminance of the LED light source is very strong. When the LED light source is transmitted using the prism structure only, the beam is shaped into two directions as shown in Fig. 3(b)-2. In other words the prism structure has a beam splitting function, but the uniformity of luminance get low. Therefore, a cylindrical structural is used to increase the uniformity in the luminance as shown in Fig. 3(b)-3. The diffuser sheet extends the surface of the LED light source. In general, the diffuser design includes a coating of diffuser particles in the structural design. The coating allows the luminance to be relatively uniform, but the optical efficiency get low. Compared with the general diffuser, the double structural diffuser had the function of high optical efficiency and

reduction of the multi-shadow effect. Above description is the result of single LED chip working function. In this luminaires, we use 64 LED chips in our experiment. The superposition effect of 64 LED chips not only forms a good reduction of multi-shadow but also increases illumination uniformity.

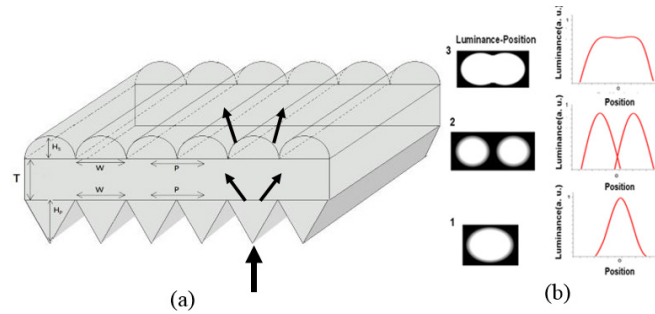


Fig. 3. Diagram showing (a) the light source passing through a diffuser sheet; (b) the luminance at different positions (1,2,3) of the diffuser sheet.

3. The optical simulation and design results of the anti-glare luminaire

3.1 Optical design flowchart

In order to design an anti-glare luminaire, the design target must be confirmed firstly. According to the specifications of a typical luminaire [3–6], we set the balanced design target for the anti-glare luminaire. The illumination uniformity should be higher than 75%, the optical efficiency should be higher than 80%, and the UGR value less than 19.0. Based on those design targets, a flowchart for the anti-glare luminaire design as shown in Fig. 4 has four main parts. First, based on the above principles the TIR surface and freeform surface are analyzed. Second, the anti-glare lens is constructed and its suitability verified by the optical software. After the illumination uniformity and the UGR satisfy our targets, the anti-glare lens is optimized for the best optical results. Third, the results of the anti-glare lens are applied in the LED module as the emitting surface light source. Using the emitting surface light source, a diffuser sheet is constructed and the luminance uniformity verified. In this paper, the illumination optimization algorithms were used with Monte Carlo methods [19] [20]. Through the optimization, the diffuser sheet has the best luminance uniformity. Finally, a completely anti-glare LED luminaire is combined using all of the components and the lighting performance verified again.

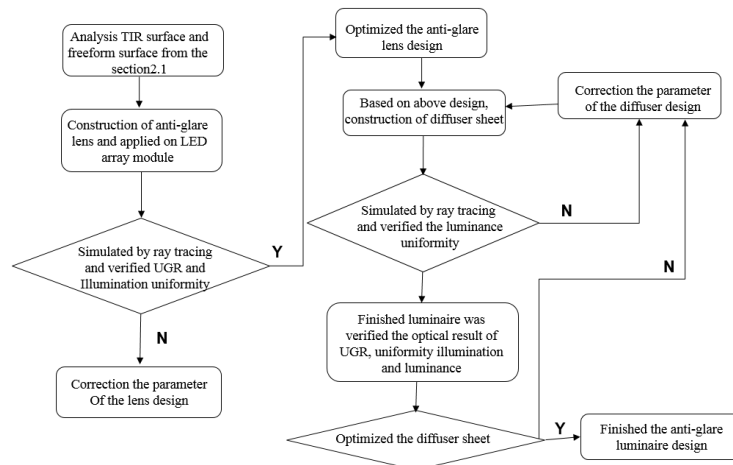


Fig. 4. The flowchart of the anti-glare luminaire design process.

3.2 Construction of the simulated anti-glare luminaire

The area of the anti-glare luminaire module was set to be 300 mm × 300 mm. The module can also be applied in different commercial lighting fixtures, for example luminaires with areas of 300 mm × 1200 mm and 600 mm × 600 mm. After the area of the luminaire was confirmed, an OSRAM-GW PSLLS1.EC was used as the light source. The LIDC of the LED source had the typical planar Lambertian distribution and the emitting surface area was 3 mm × 3 mm [21]. Then, the 8 × 8 array of LED modules was modelled by optical software of LightTools.

After the light source was designed, an anti-glare lens was constructed based on the working principles. The material used was PMMA due to its properties of high optical transmission. With Eq. (2)-(6) the radius(R) was calculated to be 5.148 mm and the angle of the lens edge (ω) was 40 degrees. Next, the freeform surface was constructed based on the above principles and using the Bezier curve to fit the radius [22]. The ray path analysis is shown in Fig. 5. The incident angle of the P1 ray path is in the range of 33 degrees. The P2 ray path passes through the spherical surface and the freeform surface. The angle of the P2 ray path is between 34 degrees and 66 degrees. The P3 ray path passes through the TIR surface to the freeform surface. When the angle of the incident ray exceeds 67 degrees, the P3 ray path is collimated by the TIR surface. The P2 and P3 ray paths also pass through the B2 surface at an angle greater than 34 degrees to be redistributed. The B2 surface and the angle of the lens edge allow a balance between the illumination uniformity and the FWHM angle of the LIDC. To achieve expected LIDC, we design the second lens with three parts (B1, B2, and TIR surface). The emitting light between 0 degree and 33 degree contain the major light flux. The B1 surface can diverge the LED emitting light between 0 degree and 33 degree for avoiding the high illumination on center. The TIR surface can reflect the emitting light over 66 degree. The TIR surface can reduce the glare effect coming from high emitting light. After deciding the TIR surface, some part of B2 surface will optimize for the light reflected by TIR surface. Finally, the emitting light between 34 degree and 66 degree can be controlled by some part of the B2 surface for batwing light distribution for high uniformity on illumination area. Moreover, the B2 surface can control the FWHM angle of LIDC. Optimization leads to great enhancement of the illumination uniformity. The FWHM angle of the LIDC is collimated at 44 degrees as shown in Fig. 5(b).

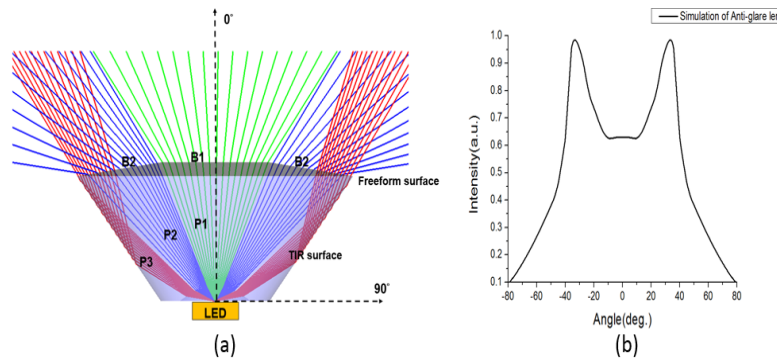


Fig. 5. (a) Ray-path analysis of the anti-glare lens; (b) LIDC of the LED with the anti-glare lens.

After the anti-glare lens was completed, the diffuser design was constructed using a prism and cylinder structure as shown in Fig. 3(a). During optimization, the prism structure was decided upon first with the beam splitting angle determined by the prism. Based on the beam splitting angle, a cylindrical structure was developed for the collimating and smooth angles. For convenience of design and manufacture, the width of the prism structure and cylinder structure were the same, making the distance of the positional shift easy to verify for manufacturing purposes. The cylinder structure was designed by the relationship between the FWHM angle and the luminance uniformity, as shown in Fig. 6. As the cylinder's ratio of

height to width increase, the FWHM angle and UGR decrease [8] and the luminance uniformity increases. The cylinder's ratio of height to width should be as higher as possible. However, our limitation of manufacture was 0.34. The diffuser design was based on this ratio to develop.

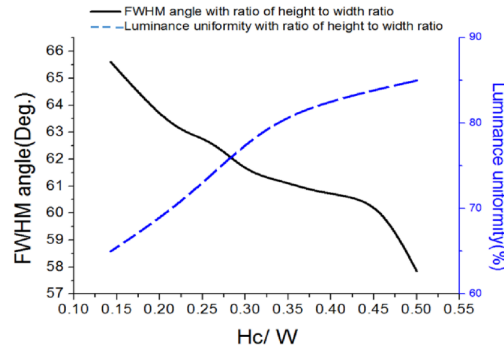


Fig. 6. Relationship between the FWHM angle and the luminance uniformity.

For optimal results, the thickness (T) of the PMMA diffuser sheet was 1mm. The prism height (H_p) was 50 μm and the cylinder height (H_C) was 23 μm . The width (W) and the pitch (P) of the two structures were 70 μm . The positional shift (ΔS) between the vertex of the prism structure and the vertex of the cylinder structure was 35 μm . The diffuser design was then applied to the LED array with the anti-glare lens. The distance between the LED light source and diffuser sheet was 5cm. The complete anti-glare luminaire design was simulated. The anti-glare luminaire not only prevented the uncomfortable glare, but also reduced the multi-shadow effect. However, the H_C and the ΔS between the vertex of the prism structure and the vertex of the cylinder structure are hard to control in the manufacturing technology of the diffuser sheet. Therefore, the tolerance analysis of the two parameters was included with in the simulation. The H_C affects the intensity angle of the anti-glare luminaire, as shown in Fig. 7(a). A higher value of H_C corresponds to a higher FWHM angle. The UGR increases with the FWHM angle. In order to control the UGR to be 19.0, the H_C should be as low as possible. In Fig. 7(b), the ΔS between the vertex of the prism structure and the vertex of the cylinder structure affects the luminance uniformity of the emitting surface. The luminance uniformity of the emitting surface occurred when the ΔS was in the range of 32 μm to 37 μm . Therefore, a ΔS of 35 μm is used as the average value in our design. For different H_C , the luminance uniformity of the emitting surface is also maintained at a high level of 35 μm although the uniformity is higher with a higher H_C . The H_C affected the angle of the FWHM of the anti-glare luminaire.

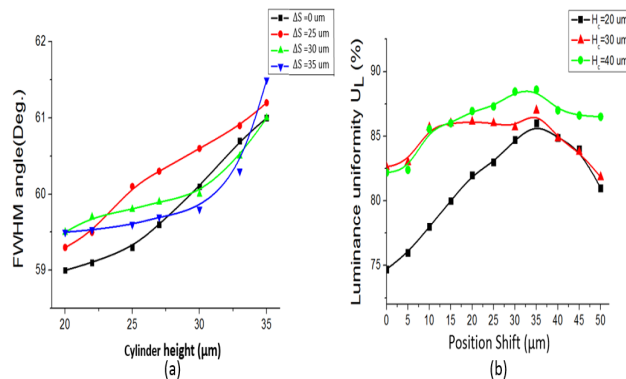


Fig. 7. (a) The tolerance between the cylinder height and FWHM angle; (b) The tolerance between the position shift and luminance uniformity.

3.3 The simulation result of anti-glare luminaire

In the beginning, the simulated traditional direct LED panel light with the LED array module had 1500 lumens and the LIDC had a Lambertian distribution. The distance between the target and the simulated luminaire was 2.15m and the target area was $2\text{m} \times 2\text{m}$. The illumination uniformity of the traditional direct LED panel light is 64.9%. The luminaire with the anti-glare lens had an intensity of 1340 lumens and batwing distribution of LIDC. There was an increase in the illumination uniformity of the luminaire with the anti-glare lens of 85.6%; see the comparison chart in Fig. 8. The illumination uniformity was enhanced from 64.9% to 85.6%. The optical efficiency was 89%.

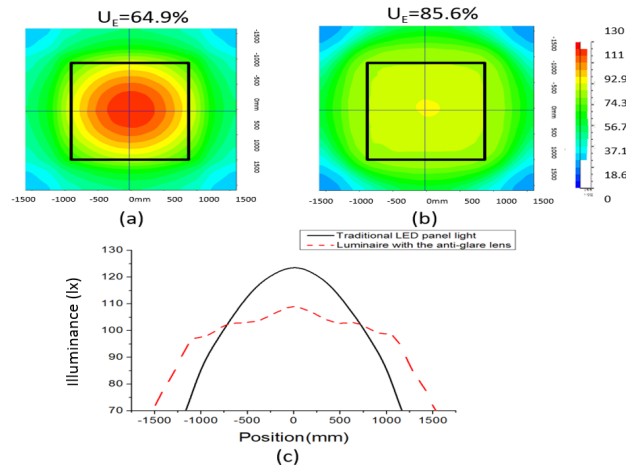


Fig. 8. Illuminance chart of (a) the traditional direct LED panel light; (b) luminaire with the anti-glare lens; (c) the comparison between (a) and (b).

For evaluation of the luminance, the viewing angle of the receiver was 0 degrees. In other words, the observer was assumed to be looking directly at the anti-glare luminaire. In Fig. 9(a), the luminance uniformity was 2%. The multi-shadow effect under the anti-glare luminaire without a diffuser was very obvious. Moreover, the luminance uniformity of the anti-glare luminaire was increased from 2% to 82.3% by adding a diffuser sheet. This phenomenon is shown in Fig. 9(b). As can be seen in the figure, the point light source with high luminance was extended to a line light source. This means that when the human eye looks directly at the anti-glare luminaire, the uncomfortable glare was reduced. The multi-shadow effect was also reduced [8, 13].

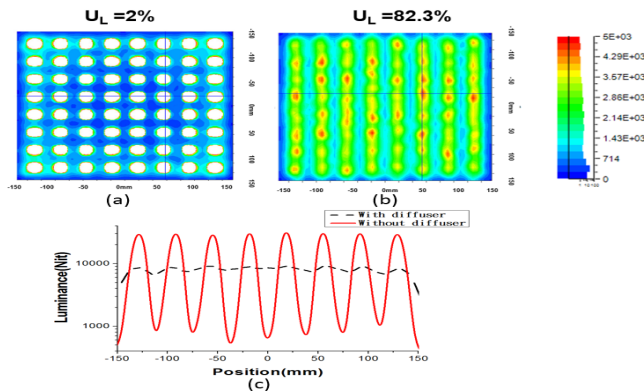
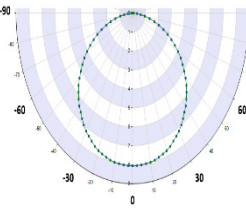
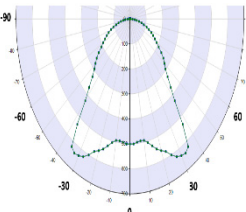
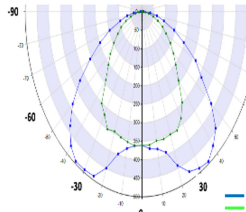


Fig. 9. Luminance chart of (a) the anti-glare luminaire without a diffuser sheet; (b) anti-glare luminaire with a diffuser sheet; (c) comparison of (a) with (b).

All design processes for the anti-glare luminaire are summarized in Table 1. In the first step, an anti-glare lens is applied to a LED array module. The illumination uniformity was enhanced from 64.9% to 85.6% and the UGR was controlled from 21.0 to 17.5. However, the luminance uniformity was low. In order to improve the luminance, a diffuser sheet was applied to complete the anti-glare luminaire. Due to this second step, the LIDC of the anti-glare luminaire was shifted in the longitudinal direction. The illumination uniformity of the anti-glare luminaire was lower than the luminaire with only an anti-glare lens. The UGR increased slightly. However, the optical targets were still remained. The optical efficiency was 79.5%, the illumination uniformity was 80.0% and the UGR was 18.8. In addition, the multi-shadow effect was reduced.

Table 1. Summary of the Anti-glare Luminaire Design Process

Type	Direct LED panel lighting	Luminaire with only an anti-glare lens	Anti-glare luminaire
Process	Basic LED array	Anti-glare lens applied in an LED array(step1)	Combined anti-glare lens and diffuser anti-glare luminaire(step2)
Lumens	1500(lm)	1340(lm)	1193(lm)
c	100%	89.3%	79.5%
U _E	64.9%	85.6%	80.0%
UGR	21.0	17.5	H18.8/ V17.8
LIDC			

4. Verification of the anti-glare lens and diffuser sheet

After working sample finished, the finished sample was tested. In order the evaluation for working sample, we adopted the normalized cross-correlation. The normalized cross-correlation (NCC) can be expressed as follows [18]:

$$NCC = \frac{\sum_i \sum_j (A_{ij} - \bar{A})(B_{ij} - \bar{B})}{[\sum_i \sum_j (A_{ij} - \bar{A})^2 \sum_i \sum_j (B_{ij} - \bar{B})^2]^{1/2}} \quad \text{Eq. (9)}$$

where A_{ij} and B_{ij} indicate the intensity of the simulated value and experimental value, respectively; \bar{A} and \bar{B} are the mean value of the simulated and experimental intensity, respectively. The precise optical model is confirmed by using the NCC.

4.1 The verification of the finished product and simulated anti-glare lens

The finished anti-glare lens is shown in Fig. 10(a). The pillars on the lens bottom are used to fix the position of the anti-glare lens. The optical performance is not influenced by the pillars because they are located below the light emitting surface of the LED. Compare the LIDC of the finished anti-glare lens with the simulation results in Fig. 10 (b). There is a difference in the LIDC of ± 10 degrees and the angle exceeds 62 degrees. Due to manufacturing defects in the spherical surface, there was a 0.2 mm shift in the distance \overline{OP} as can be seen in Fig. 2. An angle under ± 10 degrees does not diverge as in the ideal simulation. For a large difference in the angle, the pillars slightly cover the TIR surface such that the TIR was destroyed. The NCC of the LIDC can reach as high as 97.0. Due to the highly similar optics, the anti-glare lens can be considered for mass production by an injection process.

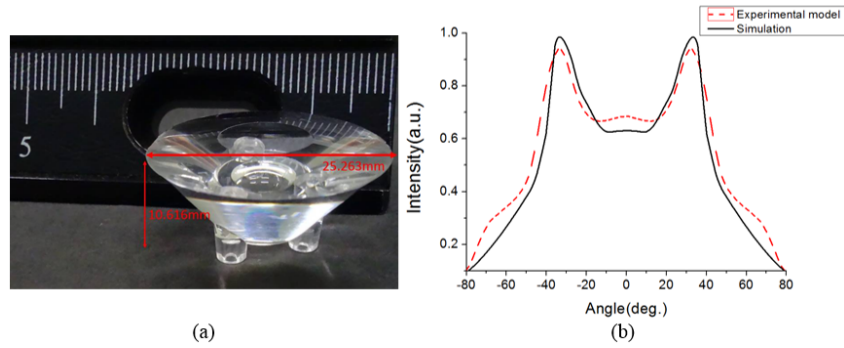


Fig. 10. (a) The finished product of the anti-glare lens; (b) Experimental results of a comparison of the anti-glare intensity distribution.

4.2 Comparison between the finished product and simulation of the diffuser sheet

The finished diffuser sheet is shown in Fig. 11. The luminaire with the anti-glare lens had high luminance as seen in the left part of Fig. 12(a). Through the correction of the diffuser sheet, the area of the light source can be extended from a point light source to a line light source as shown in the right part of Fig. 12(a). Optical measurements by luminance meters [23] show that the luminance uniformity was enhanced in one dimension from 1.3% to 87% as shown in Fig. 12(b). The diffuser sheet allows the multi-shadow effect to reduce. Figure 13(a) corresponds to the left part of Fig. 12(a). The luminaire without the diffuser sheet shows an obvious multi-shadow effect. After the application of the diffuser sheet on the luminaire, as seen in the right part of Fig. 13(a), the multi-shadow effect is reduced [13].

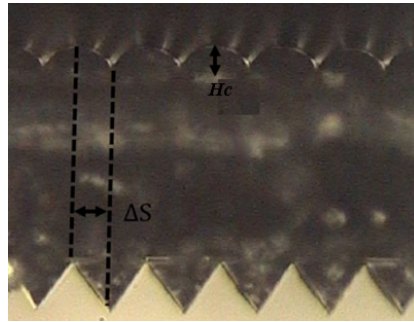


Fig. 11. The finished diffuser sheet as viewed under SEM.

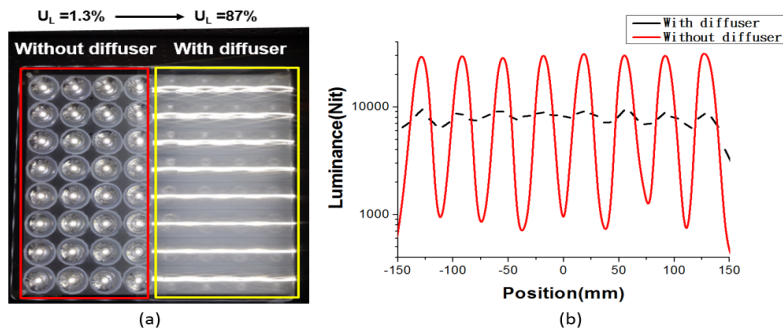


Fig. 12. (a) The finished anti-glare luminaire without the diffuser (left part outlined in red) and with the diffuser (right part outlined in yellow); (b) Experimental comparison of the luminance chart with and without the diffuser.



Fig. 13. (a) Multi-shadow effect of an anti-glare luminaire without the diffuser; (b) no multi-shadow effect with diffuser.

4.3 Verification through comparison of the finished product and simulated anti-glare luminaire

After the optical elements were verified, the completed anti-glare luminaire is shown in Fig. 14. The LIDC, luminous flux, illumination distribution, UGR optical performance, optical efficiency and illumination uniformity were measured. The LIDC, luminous flux, and the illumination distribution of an anti-glare luminaire were verified using a goniophotometer and illumination meter [24, 25]. After the measurements, the UGR and illumination uniformity were calculated using the experimental LIDC and illumination distribution. The optical flux for an anti-glare luminaire was 1140 lm under power consumption of 14 W. The experimental LIDC for 0 degrees and 90 degrees are shown in Figs. 15(a) and (b), respectively. Comparison of the NCC between the finished product and simulated anti-glare luminaire show an NCC of 95.2% for 0 degrees and 95.5% for 90 degrees. The UGR of the finished luminaire was 19.0. The illumination uniformity of the finished luminaire was 77.0%. Comparison of the optical results for the finished product with the simulated anti-glare luminaire show a reduction in the total luminous power of 53 lumens, an increase in the UGR by 0.2 and reduction in the illumination uniformity by 3%. These differences in values between the simulation and the finished product were caused by manufacturing errors in the diffuser, as shown in Fig. 7(a). As a consequence, the FWHM angle increased leading to the difference in the optical results between the simulation and the finished product. On the whole, the results for the finished product were very close to our simulation results meaning the design is acceptable for commercial lighting [3–6].

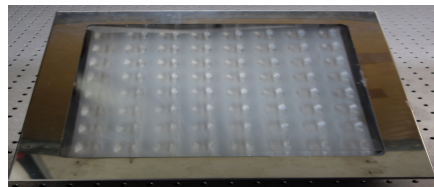


Fig. 14. The finished anti-glare luminaire.

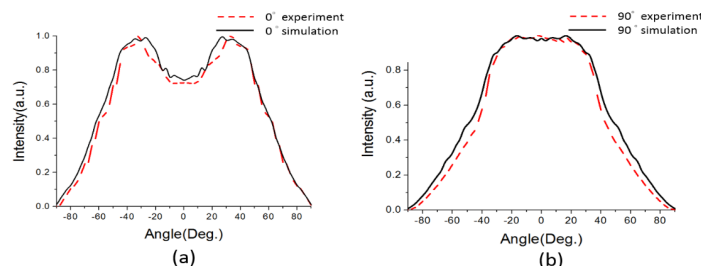


Fig. 15. Comparison of LIDC with angles of (a) 0 degrees and (b) 90 degrees between the finished product and the simulation.

4.3 Comparison of an anti-glare luminaire with commercially produced luminaires

Finally, we compare the luminaire efficacy (lm/w), UGR, and illumination uniformity between an anti-glare luminaire and commercial luminaire in the same environment with an average illumination larger than 500 lx. The measurement environment can be shown in Fig. 16. The illumination uniformity is calculated for a table with an area of 3 m × 2 m. As shown in Table 2, the luminaire efficiency for the traditional fluorescent luminaire [3] was 70.9 lm/w, the illumination uniformity on the table was 75.0%, and UGR was 16.5. For the edge-lit LED luminaire [6], the luminaire efficacy was 74.1 lm/w, the illumination uniformity on table was 76.4%, and the UGR was 18.8. For direct LED luminaire [4], the luminaire efficacy was 83 lm/w, the illumination uniformity on the table was 83.2%, and the UGR was 21.0. For our anti-glare luminaire design, the red rectangle was the target area by 3 m × 2 m and useful optical flux was 1340 lumens. The luminaire efficacy was 81.4 lm/w, the illumination uniformity on the table was 78.3%, and the UGR was controlled at 19.0.

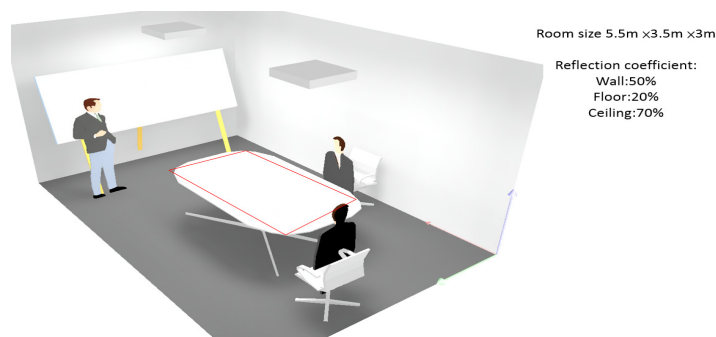


Fig. 16. Comparison office space environment.

Table 2. Comparison between an Anti-glare Luminaire and Commercial Luminaires

Type	Fluorescent Luminaire	Edge-lit LED luminaire	Direct LED luminaire	Anti-glare luminaire
Luminaire Efficacy (lm/w)	70.9 lm/w	74.1 lm/w	83 lm/w	81.4 lm/w
U_E	75.0%	76.4%	83.2%	78.3%
UGR	16.5	18.8	21.0	19.0

5. Conclusion

In this paper, we present an anti-glare luminaire with high optical efficiency, high illumination uniformity and acceptable UGR. In general LED luminaires suffer from a serious glare effect and multi-shadow effect. We propose an optical design for these defects by an anti-glare lens and diffuser sheet. In the simulation results the illumination uniformity was 80.0%, the UGR was 18.8 and the optical efficiency was 79.5%. For the working sample, the illumination uniformity was 77%, the UGR value was 19.0 and the optical efficiency was 76.0%. The finished product can be improved to be better than the simulation results. Comparison of our anti-glare luminaire design with the traditional luminaire shows an improvement in the optical performance. An anti-glare luminaire is very suitable for indoor lighting. It can provide high illumination uniformity and low power consumption without serious glare and multi-shadow effects.

Acknowledgments

This study was supported in part by the Energy Technology Program for Academia, Bureau of Energy, Ministry of Economic Affairs, project number 102-E0607.